Investigation of Structural, Optical and Photocatalytic Properties of Sr Doped Zno Nanoparticles

S. LAKSHMANA PERUMAL [1] P.HEMALATHA[1]
M.ALAGARA[1] K.NAVANEETHA PANDIYARAJ[2]

[1] Centre for Research and Post-graduate studies in Physics Ayya Nadar Janaki Ammal College, Sivakasi–626 124, Tamilnadu, India.
[2] Surface Engineering Laboratory, Department of physics, Sri Shakthi Institute of Engineering And Technology, Coimbatore 641062, India.   E-mail: laxmanmeera1201@gmail.com

Abstract

Pure ZnO and Sr doped ZnO nanoparticles are synthesized via Co-precipitation method using Zinc acetate dehydrate Zn (CH₃COO)₂. 2H₂O, Strontium acetate Sr (CH₃COO)₂, as source materials. The influence of Sr dopants contents on the morphology, absorption, emission, and photocatalytic activity of ZnO synthesized nanoparticles was investigated systematically. The photocatalytic activity of pure and Sr doped ZnO nanoparticles were detected by the degradation of MB under visible light were investigated. XRD results show that the diffraction peaks of the Sr doped ZnO nanoparticles were indicated, no characteristic peaks of any other impurities are detected in the patterns, which indicates that all the samples have high phase purity. The XRD peak shift arises due to the strain and crystallite size of the nanoparticles. This effect of strain can be investigated using Williamson Hall Plot. SEM images clearly reveal that the added Sr concentration is expected to influence the morphology of ZnO significantly. It can be observed that the morphology and grain size are different with respect to doping concentrations. UV-Vis analysis shows that the particles have a higher absorption in UV region with a slightly decreased of optical band gap (E_g). The photocatalytic activity of pure and Sr doped ZnO nanoparticles were detected by the degradation of MB under visible light were investigated.

Keywords: Sr doped ZnO Photocatalyst; Defects; Optical properties

Introduction

ZnO has received much attention over the past few years because it has a wide range of properties and applications. One of the prominent materials in the metal-oxide family, nanostructured ZnO has been intensely studied for its versatile physical properties and promising potential for electronics in particular optoelectronics applications (6). In this context, ZnO is a wide band gap (E_g=3.3eV) semiconductor nanoparticles, group II-VI in particular, have attracted a great deal of attention because of its luminescence and Photocatalytic properties. Generally, zinc oxide nanoparticles can exhibit unique properties due to their limited size and high surface area. Recently, how to enhance the photocatalytic activity of ZnO has drawn much attention from researchers all over the world. It is accepted that the surface area and lattice defects play important roles in photocatalytic activities of metal oxide semiconductors (5). Researchers also found that doping is an effective and facile method to improve the photocatalytic properties because the variation of the surface area, the incorporated of dopant ions is able

International Journal of Chemical and Physical Sciences, ISSN:2319-6602
IJCPS Vol. 4 Special Issue-6 APST–2015
www.ijcps.org

to generate lattice defects and variation of band gap energy. Consequently, doping of transition metals, noble metals and non-metals is a very expedient way to improve the photocatalytic activity. Many elements such as Al, Ta, Cr, La, Ag and I have been used as dopants and showed better photocatalytic performance (5).

Several techniques such as auto-combustion, sol-gel, microwave, co-precipitation, etc. have been used to synthesize ZnO NPs. Co-precipitation method is simple inexpensive and high-yield providing synthesis of ZnO NPs. In the present investigation, we have studied ZnO NPs synthesized by simple co-precipitation method using Scanning electron microscope (SEM), X-ray diffraction (XRD), FTIR spectroscopy, Optical absorption (UV-Vis), photocatalytic spectroscopy (PL), and photocatalytic measurements. Similar studies have also been done for pure and Sr doped ZnO NPs annealed at 400^0C.

Experimental Details

Source and materials

The starting materials used in this experiment were analytical without further purification. Zinc acetate dehydrate Zn $(CH_3COO)_2.2H_2O$, Strontium acetate Sr $(CH_3COO)_2,$ Sodium hydroxide NaOH (pellets), Ethylene glycol $(C_6H_6O_2)$, Methylene Blue (MB) dye, distilled water, and ethanol as source of materials.

Preparation of pure ZnO and Sr doped ZnO

Pure ZnO and Sr doped ZnO nanoparticles are synthesized via co-precipitation method. A typical synthesis route was as follows: Initially, (0.2M) of Zinc acetate dehydrate was dissolved in 50ml of distilled water and 10ml of ethylene glycol $(C_6H_6O_2)$ was added, The obtained solution was stirred constantly using the magnetic stirred for 2 hours. The 50 ml of Sodium hydroxide (0.2M) solution was added drop by drop to the above solution with stirrer and heated at 60^0 C for 1 hr, the Zn $(OH)_2$ precipitation was obtained. After the reaction was terminated and cooled down to room temperature, the prepared white precipitated was collected. Thus obtained nanoparticles were washed more than 3 times using distilled water and ethanol. After washing the nanoparticles were dried using hoter air oven at 80^0C for 1 hr. Finally the sample is kept calcinations at 400^0C for 1hr.

For the preparation of Sr-doped ZnO nanoparticles, different concentrations of Strontium acetate (0.2g, 0.4g) were put into 50ml Zinc (0.2mol/L) solution separately. The next steps of the preparation of Sr-doped ZnO nanoparticles remain as the same as the preparation of pure ZnO nanoparticles introduced above.

Measurement of Photocatalytic activity

The Photocatalytic activity of the Pure and Sr doped ZnO nanoparticles were evaluated by using Methylene blue (MB) under the natural solar light irradiation. In a typical procedure, a mixture of 50 ml of MB solution and 0.05g of the Pure and Sr doped ZnO nanoparticles was separately stirred for 20

International Journal of Chemical and Physical Sciences, ISSN:2319-6602
IJCPS Vol. 4 Special Issue-6 APST–2015
www.ijcps.org

min, to reach adsorption / desorption equilibrium in the dark. The solution was directly irradiated under natural solar light with similar conditions on sunny days of March- April between times of 0min, 60 min, 120min and 180min respectively and the sun's rays were very intense in this period in the city of Sivakasi. At different intervals of time, samples were taken from the suspensions. The solutions were centrifuged and the supernatant solution was collected for the determination of concentrations for the remaining dye by measuring its absorbance (at λ_{max}=660nm) with visible spectrophotometer. The photocatalytic degradation (PCD) efficiency (η) was calculated from the following expression

$\eta = \dfrac{C_{i-}C_{t}}{C_i}$ ₓ% Where C_i initial concentration and of MB and C_t is concentration of MB after "t" minutes.

Results and discussion

XRD Analysis

Figure (1.a) shows the XRD patterns of pure ZnO and Sr doped ZnO nanoparticles synthesized by Co-precipitation method. The peaks at 2θ of 31.8, 34.48, 36.30, 47.6, 56.65, 62.9, 66.4, 67.9, 69.1, 72.5, 77.0 corresponding to the (100) (002) (101) (102) (110) (103) (200) (112) (201) (004) (202) planes of pure hexagonal wurtzite structure of ZnO respectively (JCPDS Card number 897102), and no characteristic peaks of any other impurities are detected in the patterns, which indicates that all the samples have high phase purity. There are no peaks for the formation of metal oxide such as Sr-doped ZnO. It was observed that the peak at $2\theta = 36.4$ for Sr doped ZnO nanoparticles were slightly shifted to lower angles as shown in figure (1.b). The shifting and broadening of XRD lines with doping strongly suggest that Sr ions were successfully incorporated into the ZnO lattice site. Where λ is the wavelength of Cu kα_1 radiation (1.54Å), θ_{hkl} is the Bragg diffraction angle and (hkl) are miller indices of concerned lattice planes. n is order of diffraction (usually n=1). Further from inter-planer spacing (d_{hkl}) for the hexagonal wurtzite structure (refer equt.1)

$$\frac{1}{d_{hkl}^2} = \frac{4}{3}\left(\frac{h^2 + k^2 + hk}{a^2}\right) + \frac{l^2}{c^2} \tag{1}$$

With the first order approximation, n=1

$$sin^2\theta = \frac{\lambda^2}{4a^2}\left[\frac{4}{3}(h^2 + k^2 + hk) + \left(\frac{a}{c}\right)^2\right]$$

For the (100) orientation at $2\theta = 31.8$; the lattice constant "a" was calculated by

$$a = \frac{\lambda}{\sqrt{3}sin\theta}$$

and for the (002) orientation at $2\theta = 34.48$; the lattice constant "c" was calculated by

$$c = \frac{\lambda}{sin\theta}$$

The crystalline size and lattice parameter of pure and Sr doped ZnO nanoparticles are noted (Table 1.0) Lattice parameter of "a" and "c" of the Sr doped ZnO nanoparticles increased. It was observed that the lattice parameter increase with increase of doping concentration. This is due to the ionic radius of Strontium larger (2.45 Å) than that of Zn (0.74 Å). As the result of particle size is increase due to the doping concentration about range of 0.2g; 0.4g.The average size of the ZnO nanoparticles is measured by Debye- Scherrer formula [Equt (2)]. Hence the average crystalline size varies from 14 nm to 24nm as shown in table (1.0).

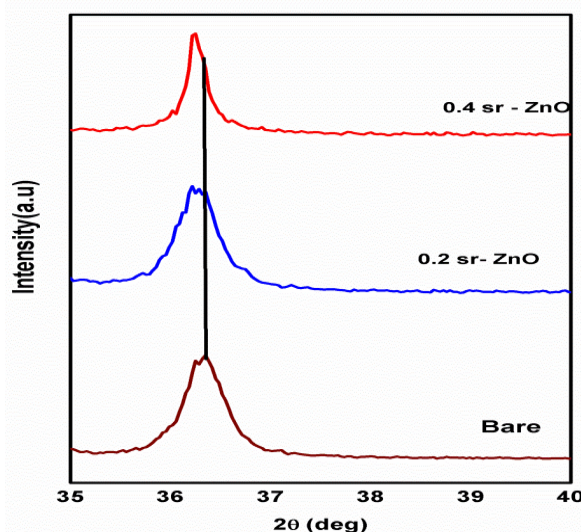$$D = \frac{k\lambda}{\beta cos\theta} \qquad \text{[Equt (2)]}$$

D is the average crystalline size; K is constant at value equal to 0.9; θ is the Bragg's angle of diffraction lines; λ is the wavelength of incident x-rays (λ=0.154nm); β is the full width at half maximum (FWHM) in radians.

W-H Plot and strain estimation

The XRD peak shift arises due to the Strain and Crystallite size of the nanoparticles. This effect of Strain can be investigated using Williamson Hall Plot. The particle size and Strain can be calculated from the intercept at the Y-Axis and slope respectively. Figure.2.a-2.c shows the W-H Plot of various doping concentration (0.0; 0.2g; 0.4g) of Strontium doped Zinc oxide nanoparticles (7).
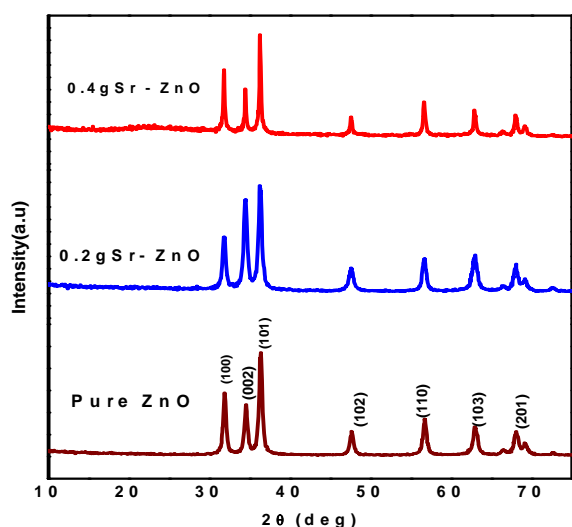
Fig.1.a XRD patterns of pure ZnO and Sr doped ZnO nanoparticles

Fig.1.b. Changes in the (101) peak position with Sr concentration.

International Journal of Chemical and Physical Sciences, ISSN:2319-6602
IJCPS Vol. 4 Special Issue-6 APST–2015
www.ijcps.org

$$\beta \, Cos\theta = \left(\frac{k\lambda}{d}\right) + (2\varepsilon \, sin\theta)$$

Where, ε is the strain induced on the particles; θ is the bragg angle; d is the average grain size in nm. The graph is plotted between $sin\theta$ and $\beta cos\theta$ as shown in figure 2.a-2.c. The Strain (ε) and Particle size (d) are presented in the Table 1.0. It has been referred that the addition of doping concentration to the growing samples will contribute some strain as formed. However, as seen from W-H Plot, the strain values are very small and their effect on the peaks broadening is insignificant. The comparison between Williamson Hall Plot and Scherrer's calculation for the particle size determination. It was observed that the particle size is found to be larger than the size reported using Scherrer's formula. Thus there is a slight variation in the particle size when compared with the effective particle size taking the strain into account obtained from W-H Plot.
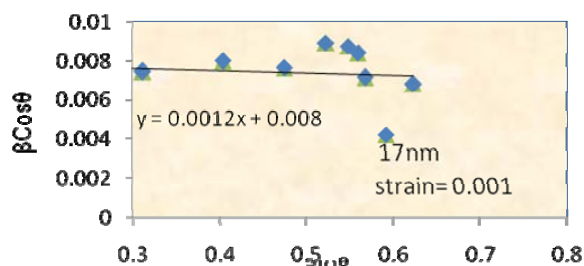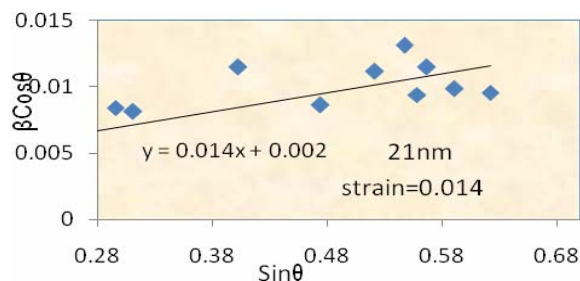

Figure.2.a. W-H Plot of pure ZnO nanoparticles

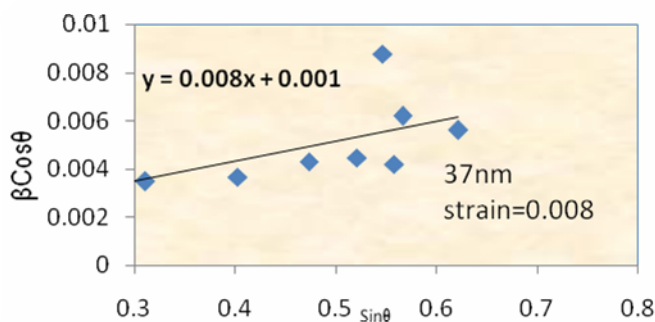**Figure.2.b.** W-H Plot of 0.2g Sr doped ZnO nanoparticles

Figure.2.c W-H Plot of 0.4g Sr doped ZnO nanoparticles

Table 1 Geometric parameters of pure and Strontium doped ZnO nanoparticles

Samples	Particle Size by Debye Scherrer (nm)	Lattice Parameter		Particle Size by W-H Plot (nm)	Band gap (eV)	Strain ε
		a (Å)	c (Å)			
Pure ZnO	14	3.246	5.197	17	3.15	0.001
0.2g Sr-ZnO	16	3.249	5.207	21	3.10	0.014
0.4g Sr-ZnO	24	3.251	5.210	37	3.0	0.008

International Journal of Chemical and Physical Sciences, ISSN:2319-6602
IJCPS Vol. 4 Special Issue-6 APST–2015
www.ijcps.org

Morphology and structural analysis

Scanning Electron Microscopy (SEM) is one of most widely used techeniques in characterization of nanomatrials. The surface morphology of the perpared nanoparticles is identified by SEM measurements. SEM images of the synthesized pure ZnO and Sr doped ZnO nanoparticles are shown in fig 3.a-3.c. It can be seen that ZnO nanoparticles was successfully synthesized. The surface morphology of the prepared pure and Sr doped ZnO nanoparticles are looks like cubic. SEM images clearly reveal that the added Sr concentration is expected to influence the morphology of ZnO significantly. It can be observed that the morphology and grain size are different with respect to doping concentrations. The pure ZnO nanoparticles are more easily to agglomerate as shown in fig (3.a). The agglomeration probelm of pure ZnO can be solved by increase doping Sr concentration as shown in fig (3.b) & (3.c).
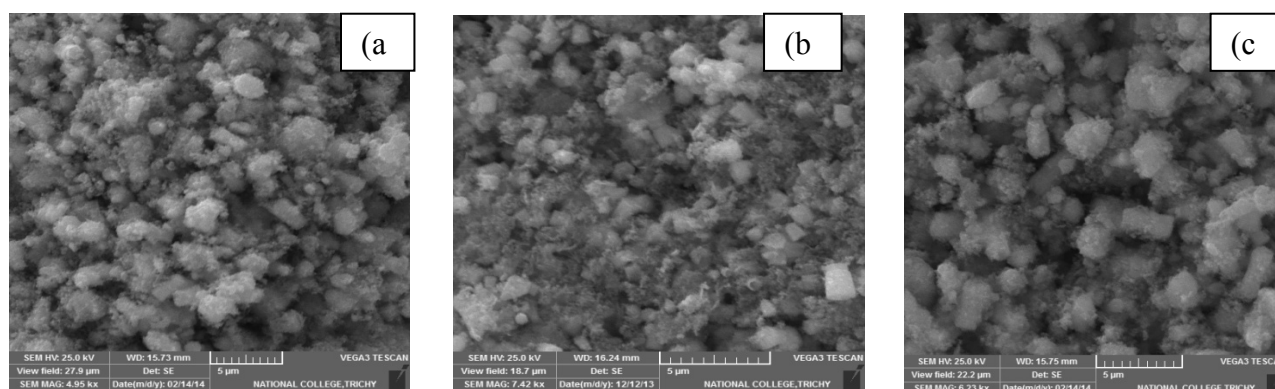

Figure.3.a-3c SEM images of (a) Pure ZnO (b) 0.2g of Sr doped-ZnO (c) 0.4g of Sr doped-ZnO.

Optical absorption Studies

UV- Vis absorption spectral analysis is used to probe the band structure of materials. The UV absorption spectra of Pure ZnO and Sr doped ZnO as functions of wavelength are shown in figure.4.0. It can be seen that there exists a strong absorption Edge below 410nm for all samples. The absorbance of Sr doped ZnO nanoparticles are shifted towards higher wavelength than pure ZnO nanoparticles. There is a significant change in the amount of absorbance due to the introduction of Strontium atom into ZnO lattice.

For the direct transition, the optical band gap energy of pure ZnO and Sr doped ZnO nanoparticles is determined using the Tauc-plot relation (8) **$\alpha\ h\upsilon = c\ (h\upsilon - E_g)^n$** where, $h\upsilon$ is the photon energy in eV, E_g is the optical band gap in eV, C is constant, and n characterizes the nature of transition. The value of n may be 1/2, 2, 3/2, and 3 for allowed direct, allowed indirect, forbidden direct, forbidden indirect transition respectively. The calculated band gap energy of undoped and doped ZnO nanoparticles comes out to be 3.15eV, 3.10eV, 3.0eV for pure ZnO, 0.2g Sr-doped ZnO, 0.4g Sr-doped ZnO respectively. Clearly, the band gap decreases slightly with the increasing of Sr-doping concentrations. The

International Journal of Chemical and Physical Sciences, ISSN:2319-6602
IJCPS Vol. 4 Special Issue-6 APST–2015
www.ijcps.org

shift of band gap may result from the change of ZnO lattice distortion. It can generate more defects in the ZnO lattice and result in the change in absorption of light and photocatalytic performance (5). In addition, when the Sr doping concentration reaches 0.4g, the ZnO exhibits the smallest band gap of the corresponding best absorption ability in visible-light region.
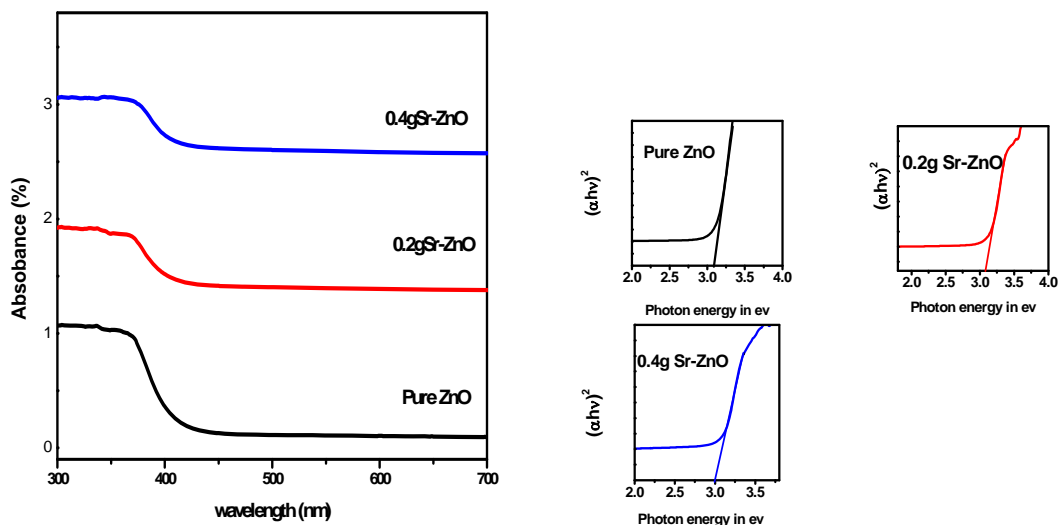

Figure.4.0. UV-Vis absorption spectra and band gap determination of the pure and Sr-doped ZnO nanoparticles.

Photoluminescence Spectroscopy (PL)

Photoluminescence spectrum (PL) study of Sr-doped ZnO nanoparticles provides valuable information about the quality of the materials and presence of intermediate transition are well described in PL spectra. PL spectra of the pure ZnO and Sr-doped ZnO nanoparticles are shown in Fig.5.0. PL results therefore can be employed to predict the defect responsible for controlling the optical and electronic property of ZnO nanoparticles. The strong UV region peak corresponding 390nm may be attributed exciton recombination related near band edge emission of ZnO. Other peaks cantered at 450nm, 490nm, and 520nm are also observed. Many researchers show that the Zinc interstitials, Zinc vacancies, and oxygen vacancies are responsible for the visible emission (8). The Blue emission at 450nm and blue-green band emission at 490nm are ascribed to surface defects. The green emission at 520nm may be assigned to oxygen vacancy (8). However, our results show that oxygen vacancies are responsible for green emission. The low intensity of the green emission may be due to the low density of oxygen vacancies during the preparation of pure ZnO and Sr-doped ZnO samples. It's well accepted fact that presence of defects in nanoparticles of ZnO is manifested by their defect related visible emission in the blue-green region. In this section the defects responsible for visible luminescence in ZnO nanoparticles and their possible location have been investigated.

Therefore, certain relationships between PL intensity and photocatalytic activity can be revealed on the basis of PL attributes. Thus, it can be suggested that oxygen vacancies and defects are in favor of photocatalytic reactions and the stronger the excitonic PL spectrum, the larger the content of oxygen vacancy or defect, and the higher the photocatalytic activity (10).
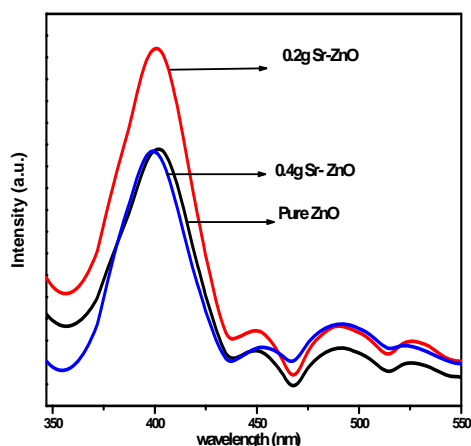
Fig.5.0 PL spectra of pure and Sr-doped ZnO nanoparticles
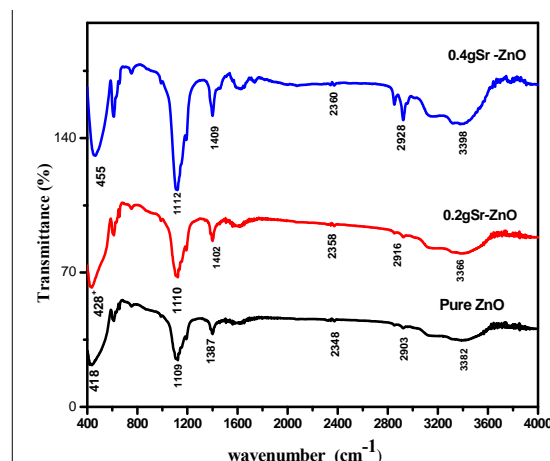
Fig.6.0.FT-IR Transmission spectra of pure and Sr-doped ZnO Nps

Fourier Transform Infrared Spectroscopy (FTIR)

FTIR measurements are taken in order to identify any absorbed species on to the particle surface. In region between $4000cm^{-1}$-$400cm^{-1}$ both stretching and bending modes give rise to absorption. If the frequency of the bond between the two atoms is high, the frequency of vibration is also high. The FTIR Spectra of Pure ZnO and Sr doped ZnO nanoparticles are shown in figure 6.0.The peak of Zn-O vibration gives an intense, broad band between 1000 and $400cm^{-1}$. The water surface of ZnO nanoparticles gives a broad envelope around $3400cm^{-1}$ Since, we have used water as solvent in our synthesis, the OH Stretching occurred predominantly. The vibration peaks at $3398cm^{-1}$, $3386cm^{-1}$, $3382.7cm^{-1}$ indicating the OH-Stretching and $1409cm^{-1}$,$1112cm^{-1}$ suggests the absorption of ethylene glycol molecules on the surface of ZnO nanoparticles (7). The band occurring at $2360cm^{-1}$, $2258cm^{-1}$ corresponding to the absorbance of CO_2 in the process of sample preparation. In the figure, sharp distinct vibrational bands at $600cm^{-1}$ and $400cm^{-1}$ are observed and attributed to the Zn-O Stretching vibration. Sr-O vibration was reported to occur at $200cm^{-1}$(22). Here, the spectra presented in fig are recorded between $400cm^{-1}$ and $4000cm^{-1}$ .Where in the Sr-O Vibration is not shown. The peak is shifted to higher wave number in all spectra of Sr doped ZnO nanoparticles and this is taken as evidence for Sr interaction with ZnO (9).

International Journal of Chemical and Physical Sciences, ISSN:2319-6602
IJCPS Vol. 4 Special Issue-6 APST–2015
www.ijcps.org

Photocatalytic Activity of Pure and Sr Doped ZnO nanoparticles

The photocatalytic activity of pure and Sr doped ZnO nanoparticles were detected by the degradation of MB under visible light is shown in figure.7.0. In this present work, the photocatalytic activity increases with an increase in Strontium concentration. The higher doping concentration of 0.4g Sr doped ZnO as shown the best photocatalytic activity among all of the synthesized ZnO nanoparticles. Hence, the shown Table.2 Order of the photocatalytic activities of the 0.4g Sr doped ZnO photocatalyst exhibits with MB concentration reduced by as much as 97% after 180 min irradiation. The detailed results of the adsorption spectra during the photocatalytic degradation process of 0.4g Sr doped ZnO are displayed in figure.7.0. This is due to the band gap plays an important role in deciding the photocatalytic activity of photocatalyst for the reason that it participates in determining the e^-/h^+ recombination rate. The band gap was measured from diffuse reflectance absorption spectrum. The band gap energy was decreased when the Sr content was increased. Thus, 0.4g Sr doped ZnO nanoparticles were selected as best photocatalyst for the study of other parameters.
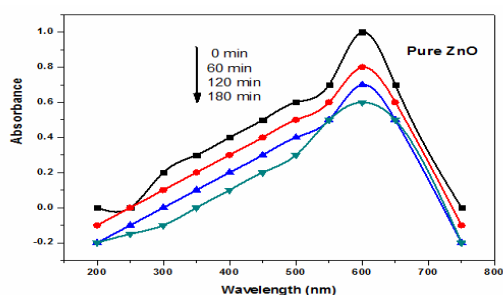

Fig.7(a) Visible absorption spectra of MB after different irradiation time using Pure ZnO
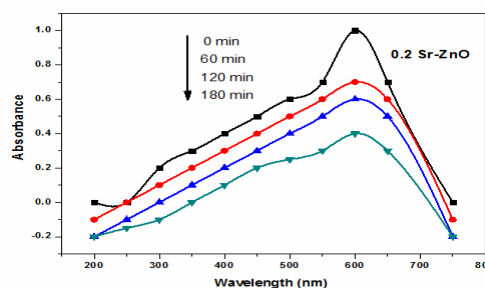

Fig.7(b) Visible absorption spectra of MB after different irradiation time using 0.2g Sr doped ZnO
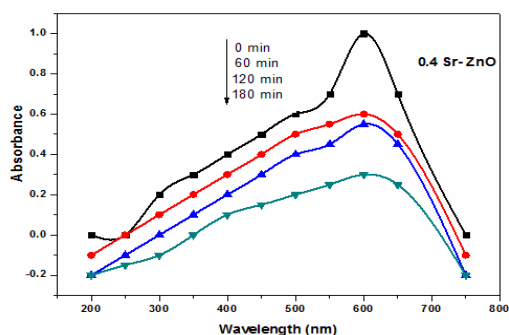

Fig.7.0 Visible absorption spectra of MB after different irradiation time using 0.4g Sr doped ZnO nanoparticles as photicatalysts
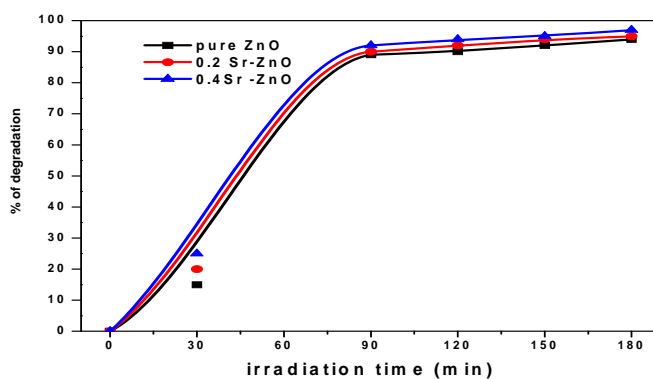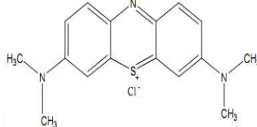

Figure.8.0. Effect of illumination Time on PCD Efficiency (experimental condition MB=10ppm, Photocatalysts= 50mg/50ml, λ=660nm)

International Journal of Chemical and Physical Sciences, ISSN:2319-6602
IJCPS Vol. 4 Special Issue-6 APST–2015
www.ijcps.org

Table.2 Shows pure and Sr doped ZnO nanoparticles of the PCD Efficiency (η) at 180 min.

Molecular Structure	Name of the Dye	Irradiation Light	Sample	PCD Efficiency at180 min
	Methylene Blue	**Sun Light**	Pure ZnO	**94%**
			0.2 Sr-ZnO	**95%**
			0.4 Sr-ZnO	**97%**

### *Effect of Surface defects on the photocatalytic activity*

Photocatalytic activity is highly related to the concentration of defects on the surface of the nanomaterials. Influences of defects have been proposed in the literature for the enhanced photocatalytic activity of ZnO [14]. Usually, higher photocatalytic activity of ZnO nanoparticles has been attributed to the high concentration of surface defects (oxygen vacancies and zinc interstitials).

Effect of illumination Time

Figure.8.0. shows the photocatalytic degradation of an MB solution as a function of the irradiation time on the pure and Sr doped ZnO nanoparticles prepared by the co precipitation method. The photocatalytic efficiency depended on the irradiation time because the MB molecules can become more oxidized with a longer irradiation time

Mechanism of Semiconductor Photocatalysis

When a semiconductor nanoparticle is irradiated by the light of energy higher or equal to the band gap energy, an electron from the VB is excited to the CB with simultaneous generation of a hole (h^+) in the VB. Then the defects benefit the efficient separation of the generation of the (e^-/h^+) pairs, The photo generated electrons reacted with O_2 or oxygen species to produce super oxide anion radicals (O_2^-) whereas the photo generate holes react with water molecules to generate the hydroxyl radicals (OH). Both radicals are oxidizing species in the photocatalytic oxidation processes. During the photocatalytic process the hydroxyl is recognized to be the most powerful oxidizing species which can attack organic pollutants at are near the surface of photocatalyst and make them into water and CO_2. High charge separation rate is beneficial to form hydroxyl radical, which favors the decolorization of MB. It can be concluded that more active defect sites may provide much help to improve products photocatalytic properties [5]. Figure.9. shows the schematic diagram of photocatalytic reaction of on illuminated semiconductor nanoparticles.
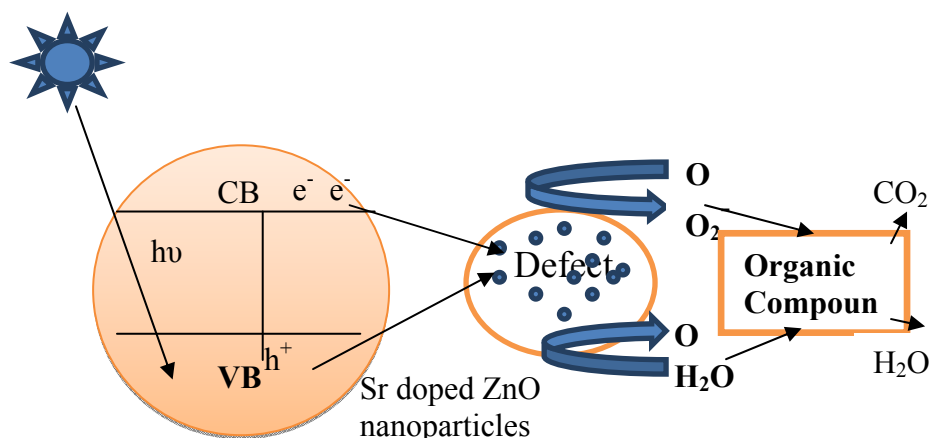
Figure.9. Shows the schematic diagram of photocatalytic Mechanism
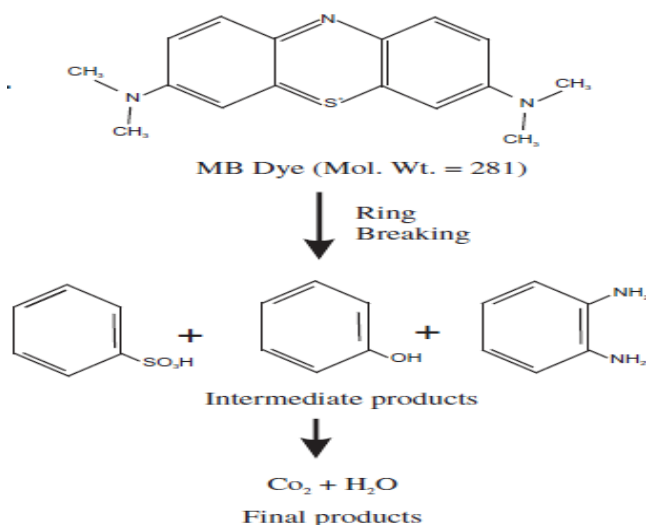
Photocatalytic degradation path way of MB.

Conclusion

Semiconductors have been widely investigated and are promising materials for efficient photocatalytic degradation. Generally, zinc oxide nanoparticles can exhibit unique properties due to their limited size and high surface area. In this present work, ZnO nanoparticles are successfully synthesized by Co-precipitation method and tries to reveal their photocatalytic activity under sun light irradiation. XRD results was observed that the peak shifting and broadening of XRD lines with doping strongly suggest that Sr ions were successfully incorporated into the ZnO lattice site. The XRD peak shift arises due to the Strain and crystallite size of the nanoparticles. This effect of strain can be investigated using Williamson Hall Plot. The optical band gap of ZnO NPs is found to decrease with increase Sr doping concentrations. PL spectra show UV, blue, green emissions. The Zinc interstitials, Zinc vacancies and

International Journal of Chemical and Physical Sciences, ISSN:2319-6602
IJCPS Vol. 4 Special Issue-6 APST–2015
www.ijcps.org

oxygen vacancies are responsible for the visible emission. Moreover, the Sr doped ZnO crystallites are found to have enhanced photocatalytic activity than pure ZnO under sun light irradiation. Among the various applications of ZnO nanoparticles, photocatalysis is the most important application for the environmental protection.

Reference

[1]   M.A. Shah, Tokeer Ahmad, Principles of Nanoscience and Nanotechnology (2008)

[2]   Mick Wilson, Kamali Kannangara, Geoff smith and Michette Simmons, Nanotechnology Basic science and emerging technology (2004).

[3]   D.C. Agarwal, Nucl. Instrum Methods phys. Res. B 244 (2006) 136.

[4]   Ruh Ullah, Joydeep Dutta, photocatalytic degradation of organic dyes with Mn doped ZnO nanoparticles 156 (2008) 194-200.

[5]   Danli, Jian-Feng Huang, Li-Yun Cao, Microwave hydrothermal synthesis of Sr doped ZnO Crystallites with enhanced photocatalytic properties. Ceramics International 40(2014) 2647-2653

[6]   N. Rajeswari Yogamalar, R. Srinivasan, A. Chandra Bose, Multi capping agents in size confinement of ZnO nanostructured particles optical materials 31(2009) 1570-1574.

[7]   N. Rajeswari Yogamalar A. Chandra Bose, Burstein- Moss shift and room temperature Near-band–edge luminescence in lithium doped ZnO Appl phys (2011) 103:33-42

[8]   Ram Kripal, Rajneesh K.Srivastava, Photoconductivity and photoluminescence of ZnO nanoparticles synthesized via Co-precipitation method Spectro chem Acta part A 79 (2011)1605-1612.

[9]   L. Kumaresan, M. Mahalakshmi, M. Palanichamy, Synthesis, characterization and photocatalytic activity of Sr doped TiO2 nanoplates Ind.Eng.Chem.res.2010, 49, 1480-1485.

[10] Jing Liqiang, Quyichun, Wang Baiqi, Review of photoluminescence performance of nano-sized semiconductor materials and its relationships with photocatalytic activity, solar energy materials & solar cells 90 (2006) 1773-1787.

[11] N.Clament Sagaya Selvam, J. Judith Vijaya, L.Jojn Kennedy, Compartive studies on influence of morphology and La doping on structural, optical and photocatalytic properties of ZnO nano structures, Journal of colloid and interface sci 407(2013)215-224.

[12]   F.Hashemzadeh, R.Rahimi, A.Gaffarinejad, Photocatalytic Degradation of Methylene blue and Rhodamine B dyes by Niobium Oxide Nanoparticles synthesized Via Hydrothermal method. Vol. 1, No. 7, August 2013, PP: 95-102, ISSN: 2328-2827

[13]   N. Rajeswari Yogamalar, Arumugam Chandra Bose, Tuning the aspect ratio of hydrothermally grown ZnO by choice of precursor Journal of Solid State Chemistry 184 (2011) 12–20.

[14] Mu Yaoguo, Alan Man Ching, Fangzhou Liu, Effect of native defects on photocatalytic properties of ZnO phys. (2011) 115 11095- 11101.

[15] Ke Dai, Tianyou Peng, Haochen, Juan Liv, Photocatalytic degradation of commercial phoxim over La doped TiO2 nanoparticles in aqueous suspension. Eviron, scien Tech 2009, 43, 1540-1545.

[16] Xiaoqing, Quiu, Liping Li, Jing Zheng, Junjie, Liu, Origin of the enhanced photocatalytic activities of semiconductors, a case study of ZnO doped Mg2+ J.phys.chem (2008) 12242-12248.

[17] Xiaoyong Wu, Shu Yin, Qiang Dong, Chongshen Guo, photocatalytic properties of Nd and C co-doped TiO2 with the whole range visible light absorption. Phys. chem 20103 8345- 8352.

[18]   W.K. Hong, J.I. Sohn, D.K. Hwang, S.S. Kwon, G. Jo,   S. Song, S.M. Kim, T. Park, Nano Lett, 8 (2008) 950.

[19]   Nazar Elamin, Ammar Elsanousi, Synthesis of ZnO Nanostructures and their Photocatalytic Activity Journal of Applied and Industrial Sciences, April, 2013, 1 (1): 35

[20] M. Nirmala, Manjula G. Nair, K. Rekha, Anukaliani, Photocatalytic Activity of ZnO nanopowders Synthesized by DC Thermal Plasma, African Journal of Basic &Applied Sciences 2 (5-6): 161-166, 2010 ISSN 2079-2034

[21] Farantos, S.C Filippou, E.Stamtiadis, spectra of Sr Co complex: Experiment and Absorption calculation chem Lett 2002,366 231-237.

[22] N. Clament Sagaya Selvam, J. Judith Vijaya, and L. John Kennedy, Effects of Morphology and Zr Doping on Structural, Optical, and Photocatalytic Properties of ZnO Nanostructures. 10.1021/3016945 | Ind. Eng. Chem. Res. 2012, 51, 16333−16345

[23] Choi, W. Termin, A. Hoffmann, The role of metal ion dopants in quantum-sized TiO2 correlation between photocatalytic and charge carrier recombination dynamics. J. phys.1994, 98 13669-1367

[24] M.Ratner and D. Ratner, Nanotechnology -A Gentle Introduction to the next big idea, 2nd edition, (1999).

[25] James R. Connolly, Introduction to X-Ray Powder Diffraction, spring (2007).

[26] P.S.Sindhu, Elements of Molecular Spectroscopy, (2006).

[27] Manikandan, J.Judith Vijaya, L.John Kennedy, M.Bououdina, Microwave combustion synthesis, structural, optical and magnetic properties of Zn1-x Srx Fe2O4 nanoparticle. Ceramics International 39 (2013) 5909–5917.

[28] Amrut J. Sharma Raghu Mani S. Ningthoujam, J.S. Ahn Ramchandra B. Pode Low, Temperature dielectric studies of zinc oxide (ZnO) nanoparticles prepared by Precipitation method Advanced Powder Technology 24 (2013) 331–335.

[29] R. Srinivasan, N., R. Rajeswari Yogamalar Justin Josephus A. Chandra Bose, Estimation of lattice Strain, stress, Energy density and Crystallite size of the spherical Yttrium oxide nanoparticles. Department of Physics, National Institute of Technology,   Tiruchirappalli, India Received February 2009.

[30] T. Busgen, M. Hilgendorff, S. Irsen, F. Wilhelm, A.Rogalev, phys.chem 112 (2008)2412.